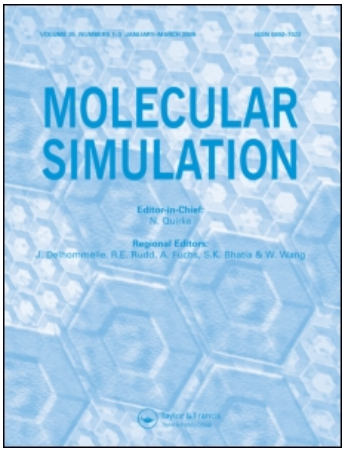

Molecular Simulation

Publication details, including instructions for authors and subscription information:
http://www.informaworld.com/smpp/title~content=t713644482

The multi-particle sampling method in Monte Carlo simulations on fluids and its efficient implementations

Filip Moučka[a]; Ivo Nezbeda[ab]
[a] Faculty of Science, J.E. Purkinje University, Ústí nad Labem, Czech Republic [b] E. Hala Laboratory of Thermodynamics, Institute of Chemical Process Fundamentals, Academy of Sciences, Prague, Czech Republic

Online publication date: 03 August 2010

To cite this Article Moučka, Filip and Nezbeda, Ivo(2010) 'The multi-particle sampling method in Monte Carlo simulations on fluids and its efficient implementations', Molecular Simulation, 36: 7, 526 — 534
To link to this Article: DOI: 10.1080/08927021003692547
URL: http://dx.doi.org/10.1080/08927021003692547

Molecular Simulation
Vol. 36, Nos. 7–8, June–July 2010, 526–534

Taylor & Francis
Taylor & Francis Group

The multi-particle sampling method in Monte Carlo simulations on fluids and its efficient implementations

Filip Moučka[a] and Ivo Nezbeda[ab]*

[a]*Faculty of Science, J.E. Purkinje University, 400 96 Ústí nad Labem, Czech Republic;* [b]*E. Hala Laboratory of Thermodynamics, Institute of Chemical Process Fundamentals, Academy of Sciences, 165 02 Prague 6, Czech Republic*

(*Received 21 December 2009; final version received 10 February 2010*)

Both physical and technical aspects of a recently introduced multi-particle move Monte Carlo scheme, i.e. the method based on biased simultaneous displacements/rotations of *all* particles of the system, are discussed and its efficiency is assessed by comparing various MC implementations. The method is naturally parallelisable which can make it much more efficient in comparison with the conventional one-particle move MC. This aspect of the method is also demonstrated by comparing efficiency of simulations on the Lennard-Jones fluid and the TIP4P model of water performed using different hardware, including fast performing graphics processing unit. Furthermore, selected results of a detailed analysis of the structure of water–methanol mixtures with both non-polarisable and polarisable interaction models are presented and the effect of the polarisation on the structure is analysed.

Keywords: multi-particle move MC; graphics processing unit; polarisable model; water–methanol mixture; spatial distribution functions

1. Introduction

Since its advent in 1953 [1], the Monte Carlo (MC) simulation method (along with the molecular dynamics method) has gradually become an indispensable tool in modern fundamental and applied research in many branches of science and engineering. Over the decades, a number of various methods (e.g. Gibbs ensemble) and tricks (e.g. umbrella sampling, fluctuation particle method, etc.) have been developed to address a larger spectrum of properties and problems, and to deal with more and more complex systems [2,3]. Nonetheless, perhaps surprisingly, the core of the method, the Metropolis importance sampling algorithm with a sequence of random one-particle moves (1PM), has not changed.

Viewing the MC experiment, intuitively, as a caricature of a real system, there is a big difference between this experiment and reality. Whereas in test tubes all particles (molecules) are in a perpetual motion, in the MC experiment, at one moment (step), only one particle attempts to move while all the remaining particles are motionless remaining in their position. A natural question must then be asked, if it were not more appropriate or more natural to devise a scheme in which all (or at least a larger group of particles) would move simultaneously. This question seems to have been asked from the very beginning of the existence of simulations [4] and a number of attempts have been made but without any apparent success. Solutions within the MC method have been searched both on the physical [5,6] and technical (e.g. a sort of parallelisation) [7–9] grounds. The only successful approach along this line has been a combination of MC and molecular dynamics methods, a hybrid MC (hMC), in which all particles follow the trajectory given by the equations of motion but the configurations are accepted by the probability criterion [10,11]. For a discussion of its advantages and disadvantages, see [2]; for its recent applications, see papers by Delhommelle et al. [12,13] and references therein.

There are two simple reasons why the early attempts to move more than one particle at once failed. If $\langle \mathcal{P} \rangle$ is the average probability of acceptance of 1PM for a given maximal displacement l_1, then a straightforward extension of the Metropolis algorithm to a simultaneous displacement of M particles (we are going to refer to this method as naive multi-particle method, nMPM) gives for the average probability of acceptance, $\mathcal{P}_m$, approximately,

$$\langle \mathcal{P}_m \rangle \approx \langle \mathcal{P} \rangle^M. \tag{1}$$

Since $\langle \mathcal{P} \rangle < 1$, $\langle \mathcal{P}_m \rangle$ becomes extremely small for large M (the so-called rejection catastrophe) and the method as is can thus be considered for very small samples only [6]. To avoid the rejection catastrophe (increase the acceptance probability), the maximal displacement l_1 must be reduced significantly which, in the end, leads to a very poor efficiency. Although M particles (or all particles of the system) are moved at once, the changes of configurations are so small that an extremely large number of steps would

*Corresponding author. Email: ivonez@icpf.cas.cz

ISSN 0892-7022 print/ISSN 1029-0435 online

DOI: 10.1080/08927021003692547
http://www.informaworld.com

have to be generated to sample the configuration space reasonably.

The other reason is that the nMPM approach was applied only to simple fluids, typically the Lennard-Jonesium (LJ), for which MPM methods may hardly bring any significant improvement. If only one particle is moved, then only the change of the intermolecular energy of this particle must be evaluated, i.e. the number of terms of the order N, where N is the total number of particles of the system. In the MPM method, this number of terms is proportional to N^2, it means by factor $\mathcal{O}(N)$ larger. The situation is, however, completely different if we deal with systems with non-additive interactions as, for example, with polarisable models. In this case, even if only one particle is displaced, the intermolecular energy of other particles is simultaneously affected as well. It means that the number of terms to be evaluated is now of the order N^2, which means of the same order as in the MPM scheme!

A typical example of systems with non-additive interactions are polarisable models. The problem of inefficiency of the 1PM method for polarisable models has been addressed by developing approximate methods based on physical arguments [14–16]. Moreover, to further facilitate the 1PM scheme, some technical aspects (e.g. criteria for convergence of iterations [16,17]) have been pushed to the very edge of acceptability. To overcome the inefficiency of MC simulations not only for polarisable models but also for models with non-additive interactions in general, we have recently proposed a novel MC method [18]. The method, called simply multi-particle move MC (MPM MC) scheme, does not generate displacements of particles at random but makes use of the idea of the force bias method [19], and thus considers simultaneous translations/rotations of all particles at once in the spirit of molecular dynamics (cf. a similar step going from naive MC to importance sampling MC). To be specific, the moves are biased according to the forces acting between the molecules. Feasibility of the approach and its efficiency was first demonstrated for the polarisable Stockmayer fluid [18]. Using a novel smoothing of the potential at the cut-off distance, we implemented it for two polarisable models of water [20] and then also applied it to the water–methanol mixture with a polarisable model of water to study its thermodynamic properties [21].

The goal of this paper is twofold. The primary focus is on efficient implementations of the MPM method making use of both its physical nature (parallelisation) and modern hardware (multiprocessor machines and graphics cards). We show that, even for pairwise-additive models (LJ and water), the MPM method may be faster than the 1PM method. Second, the efficiency of the MPM method makes it possible to study within a reasonable time very complex time-consuming problems; an example of such a system is the water–methanol mixture. Over the last years, a number of contradicting results have been published, earlier ones being at odds with neutron scattering data. Moreover, non-polarisable models seem to fail to reproduce the minimum in the partial molar volume of methanol at its low concentrations [22]. Usefulness of the MPM MC method is exemplified by its application to the study of the structure of this mixture with a polarisable model of water. Selected results for the structure of this mixture are presented to show the effect of polarisability.

2. The biased MPM method

To make the displacement of all particles at once efficient, the displacements (rotations) cannot be random. The MPM method starts from the known force-bias method [19], in which trial moves are biased in the direction of forces or torques acting on the molecules, and extends it to a simultaneous displacements (or rotations) of all particles. Thus, if $\mathbf{F}_k$ is the force acting on particle k to be displaced and t_m is the maximum length of any component of the translational vector, $\mathbf{t}_k$, then its components t_k^α, $\alpha = 1, 2, 3$, are generated according to the probability distribution:

$$\pi(t_k^\alpha) = \frac{\exp\left[\lambda\beta F_k^\alpha t_k^\alpha\right]}{\int_{-t_m}^{t_m} \exp\left[\lambda\beta F_k^\alpha t_k^\alpha\right] \mathrm{d}t_k^\alpha} = \frac{\exp\left[\lambda\beta F_k^\alpha t_k^\alpha\right]}{2\sinh[\lambda\beta F_k^\alpha t_m]/\lambda\beta F_k^\alpha}, \tag{2}$$

where $k = 1, \ldots, N$ and λ is a parameter whose value lies between 1/2 and 1, with $\lambda = 1/2$ being the common choice [19]. The acceptance probability of this move is:

$$\mathrm{Prob} = \min\left\{1, \exp[-\beta\Delta U]\frac{\omega^{\mathrm{new}\to\mathrm{old}}}{\omega^{\mathrm{old}\to\mathrm{new}}}\right\}, \tag{3}$$

where

$$\omega^{\mathrm{old}\to\mathrm{new}} = \prod_{\alpha=1}^{3} \frac{\lambda\beta F_k^{\alpha,\mathrm{old}} \exp[\lambda\beta F_k^{\alpha,\mathrm{old}} t_k^\alpha]}{2\sinh[\lambda\beta F_k^{\alpha,\mathrm{old}} t_m]} \tag{4}$$

and

$$\omega^{\mathrm{new}\to\mathrm{old}} = \prod_{\alpha=1}^{3} \frac{\lambda\beta F_k^{\alpha,\mathrm{new}} \exp\left[\lambda\beta F_k^{\alpha,\mathrm{new}} \left(-t_k^\alpha\right)\right]}{2\sinh\left[\lambda\beta F_k^{\alpha,\mathrm{new}} t_m\right]}, \tag{5}$$

where ΔU is the associated change in the internal energy, and $\beta = 1/k_\mathrm{B}T$, where k_B is the Boltzmann constant and T is the absolute temperature.

The above expressions, written for the conventional one-particle translational move, are easily extended to MPM (for details see the original paper [18]):

$$\omega^{\mathrm{old}\to\mathrm{new}} = \prod_{\alpha=1}^{3}\prod_{k=1}^{N} \omega_k^{\alpha,\mathrm{old}\to\mathrm{new}} \tag{6}$$

and

$$\omega^{\text{new}\to\text{old}} = \prod_{\alpha=1}^{3}\prod_{k=1}^{N} \omega_k^{\alpha,\text{new}\to\text{old}}, \tag{7}$$

and the formula for generating the translation vector is obtained by inverting Equation (2),

$$t_k^{\alpha} = \frac{\ln[\exp(-\lambda\beta F_k^{\alpha,\text{old}} t_m) + 2u_k^{\alpha}\sinh(\lambda\beta F_k^{\alpha,\text{old}} t_m)]}{\lambda\beta F_k^{\alpha,\text{old}}}, \tag{8}$$

where u_k^{α} is a random number within the interval (0,1).

A similar modification applies to the rotational move which can be implemented in a number of different ways. We implement this step by the rotation around a randomly chosen vector $\mathbf{r}_k$ whose length determines the value of the rotation angle. Thus, if $\mathbf{M}_k$ is the torque acting on particle k to be rotated and r_m is the maximum length of any component of the rotational vector $\mathbf{r}_k$, then its components are generated according to the formula:

$$r_k^{\alpha} = \frac{\ln[\exp(-\lambda\beta M_k^{\alpha,\text{old}} r_m) + 2u_k^{\alpha}\sinh(\lambda\beta M_k^{\alpha,\text{old}} r_m)]}{\lambda\beta M_k^{\alpha,\text{old}}}. \tag{9}$$

When deriving this formula, the same reasoning as for Equation (8), considering the relation $\triangle U \approx (\mathbf{M}_k \cdot \mathbf{r}_k)$ instead of $\triangle U \approx (\mathbf{F}_k \cdot \mathbf{t}_k)$, has been used. The acceptance probability is given by the same general formula as for translations, Equation (3), with F_k^{α} being replaced by M_k^{α}, t_k^{α} by r_k^{α} and t_m by r_m in Equations (4) and (5).

3. Models and simulation details

3.1 Models and long-range corrections

In this paper, we consider the common LJ potential, TIP4P model of water [23], polarisable BSV model of water [24] and KBFF model of methanol [25]. All these potentials are site–site models and their configurational energy is given by the general expression:

$$\begin{aligned} U &= U_{\text{LJ}} + U_{\text{qq}} + U_{\text{pol}} \\ &= \sum_{i<j} u_{\text{LJ},ij} + \sum_{i<j} u_{\text{qq},ij} - \frac{1}{2}\sum_i (\mathbf{p}_i \cdot \mathbf{E}_{i\text{P}}^{q}), \end{aligned} \tag{10}$$

where

$$u_{\text{LJ},ij} = 4\epsilon \sum_{\alpha,\beta}\left(\left(\frac{\sigma_{i\alpha,j\beta}}{R_{i\alpha,j\beta}}\right)^{12} - \left(\frac{\sigma_{i\alpha,j\beta}}{R_{i\alpha,j\beta}}\right)^{6}\right), \tag{11}$$

$$u_{\text{qq},ij} = \frac{1}{4\pi\varepsilon_0}\sum_{\alpha,\beta}\frac{q_{i\alpha}q_{j\beta}}{R_{i\alpha,j\beta}}. \tag{12}$$

In the above equations, $i\alpha$ denotes interaction site α of molecule i, $R_{i\alpha,j\beta} = |\mathbf{R}_{i\alpha,j\beta}|$ is the site–site separation, $\mathbf{p}_i$ is the induced dipole moment of molecule i and $\mathbf{E}_{i\text{P}}^{q}$ is the electric field at the centre of the induced dipole of molecule i originating in the Coulombic sites of the other molecules of the system. The induced dipoles are assumed to be proportional to the total electric field acting at their centres,

$$\mathbf{p}_i = \alpha\left(\mathbf{E}_{i\text{P}}^{q} + \mathbf{E}_{i\text{P}}^{p}\right), \tag{13}$$

where α is the scalar polarisability and $\mathbf{E}_{i\text{P}}^{p}$ is the electric field at the centre of the induced dipole of molecule i originating in the induced dipoles of the other molecules of the system. Except for BSV, all the considered models are non-polarisable, i.e. $U_{\text{pol}} = 0$, and their energy is thus pairwise additive. The particles of the simple LJ fluid do not bear any charge, i.e. $U_{\text{qq}} = 0$, and there is only one interaction site per molecule. The polarisable BSV model of water contains a point-induced dipole interaction site; the U_{pol} term contributing to the total interaction energy has thus to be evaluated. Since $\mathbf{E}_{i\text{P}}^{p}$ depends on $\mathbf{p}_j$, $j = 1, \ldots, N$, a self-consistent solution of Equation (13) must be found. An iterative technique is the common method to use. This is usually fast converging process with the criterion [26]

$$\max_{k=1,\ldots,N} \frac{|\mathbf{p}_k(n) - \mathbf{p}_k(n-1)|}{|\mathbf{p}_k(n)|} < 10^{-m} \tag{14}$$

used to terminate the iteration. For parameters and further details of the potentials see the original papers.

The correction due to the truncation of the long-range interactions must be applied, for which we use the reaction field method [27] with a novel smoothing [20] of the potentials in the range around the cut-off distance. The smoothing is used to enhance the acceptance ratio (due to discontinuity of the potential and forces at the cut-off distance, the maximal displacements would have to be otherwise considerably decreased to maintain a reasonably high acceptance ratio [20]). Finally, the forces and torques acting on the molecules have to be determined as they are necessary for the biased MPM MC moves. However, since they affect only the choice of subsequent configurations (walk in the configuration space) but not the thermodynamic values at equilibrium, it is not necessary to know their exact value. The forces can be calculated using the standard reaction field method without any smoothing; the non-smoothed and smoothed forces differ significantly only for low values of the cut-off distance. There is no reason to smooth the torques as the distances between the molecular reference sites and thus also the numbers of particles within the reaction field cavities do not change during rotations.

3.2 Graphics processing unit implementation

In addition to common hardware, the graphics processing unit (GPU) provides another, so far not fully utilised, potential hardware to be used. The most important difference between the CPU and GPU approaches is that the GPU is able to run many (thousands) threads simultaneously.

The codes for GPU have been written using the C programming language with NVIDIA extensions (CUDA version 2.2; http://www.nvidia.com/object/cuda_home.html). In our GPU codes, the forces, torques and energies of many particles are calculated concurrently. To be specific, the system of N particles is divided into blocks of N_t particles. The GPU processes the blocks separately and the force and torque acting on each particle, and the energy of the particle is calculated by N_p threads. Thus, the GPU must process $N \times N_p$ threads divided into $N_b = N/N_t$ blocks during each MPM MC step. The fast shared multiprocessor memory has been used to store the particle positions in the case of 512 and 1024 LJ particles only. Furthermore, we have not parallelised the random number generator which, depending on the number of particles and molecular model used, consumes a significant amount of the computational time. Single-precision floating-point operations have been used which is, in contrast to molecular dynamics, sufficient for the MPM MC algorithm. The calculations were executed on NVIDIA GTX 260 GPU and, in order to compare the performance gain, also on Intel Core 2 Quad 2.66 GHz processor (CPU). The parameters used for these simulations are given in Table 1.

Table 1. Parameters of the MPM MC simulations on the LJ fluid near its triple point and on ambient TIP4P water in an *NVT* ensemble.

N	N_t	N_p	t_m	r_m	r_c
LJ fluid					
512	32	8	0.042σ	–	4σ
1024	16	8	0.035σ	–	5σ
4096	32	2	0.026σ	–	5σ
TIP4P water					
512	4	16	0.06 Å	0.11	(9.5,10) Å
1024	16	16	0.055 Å	0.11	(11.5,12) Å
4096	8	32	0.05 Å	0.09	(11.5,12) Å

3.3 Evaluated properties and efficiency assessment

To assess efficiency of the considered methods, we have computed, in addition to the rate of the energy equilibration, dependence of the mean-squared displacement (MSD) [3], on computation time,

$$\mathrm{MSD}(t) = \frac{1}{N}\sum_{i=1}^{N} \frac{\langle |\mathbf{r}_i(t) - \mathbf{r}_i(0)|^2 \rangle}{t}, \qquad (15)$$

where $\mathbf{r}(t)$ is the position of the particle at time t, and averaging is performed over all particles of the sample. The MSD reflects mobility of the molecules during the simulation. A number of similar parameters can be measured; however, in our preceding papers [18,20], we have shown that, in the case of the molecular models considered, all of these parameters provide the same piece of information on the simulation efficiency.

To put the MPM MC into a practical use, we have applied it to a detailed study of the structure of the water–methanol mixture with a polarisable model of water. The MPM MC parallelised codes have been run on standard 8-core computational SGI AltixXE 310 nodes. Unlike the commonly used site–site correlation functions to characterise the structure, we have computed spatial distribution functions (SDFs) [28] determined as three-dimensional density distributions of hydrogen, oxygen and methyl interaction sites of the molecules in the local coordinate system linked with the reference molecule. For the measurement, the rotational transformation matrices of all particles have been stored in memory and updated after every rotation. To obtain the matrices of transformation in the local coordinate systems, the rotational transformation matrices have been inverted (transposed). We study the SDFs for all combinations of species, i.e. water–water, water–methanol, methanol–water and methanol–methanol. The SDFs are visualised using slices and isosurfaces at various values of density.

4. Results and discussion

4.1 Parallelisation and efficiency

The MPM MC method can be evidently easily parallelised using the common cluster configuration or other conventional hardware. Because of their architecture, the GPUs offer another possibility of parallelisation. To demonstrate usability of the MPM MC for computations on GPUs, we have implemented the algorithm for the LJ fluid with 512, 1024 and 4096 particles at thermodynamic conditions near its triple point ($T^* = 0.81$, $\rho^* = 0.8645$), and for the same number of particles also for the TIP4P water molecules at ambient conditions ($T = 298.16$ K, $\rho = 0.0334$ Å^{-3}), both the systems being simulated at constant N, $V$and T. The reaction field potentials have been smoothed but no smoothing has been applied to forces.

Development of the configurational energy and the MSD for the LJ fluid simulated using various methods, number of particles and hardware are shown in Figure 1. In accordance with our expectation, the MPM MC method without any parallelisation is rather inefficient for the system with the pairwise-additive configurational energy. For example, in the case of 1024 particles, the slope of the

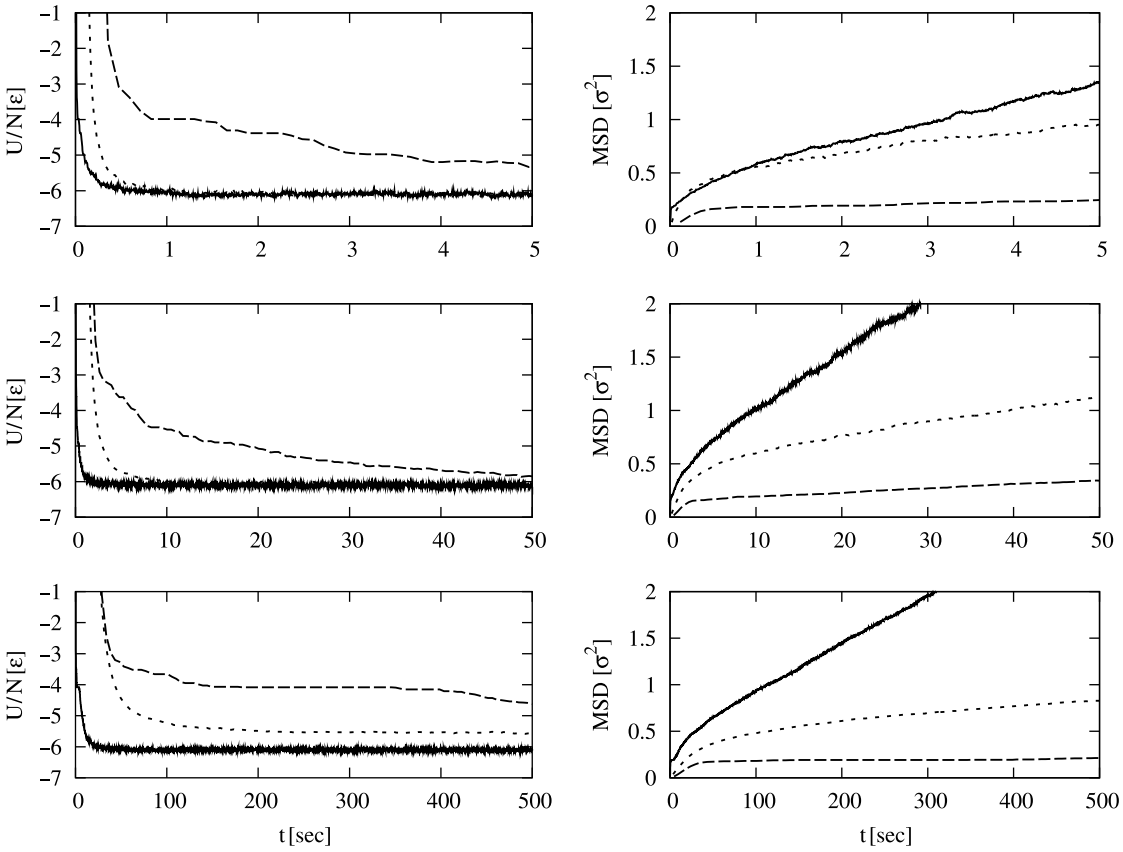

Figure 1. Comparison of the development of the configurational energy (left column) and MSD (right column) of the LJ fluid near its triple point simulated using 512 (first row), 1024 (second row), 4096 (third row) particles and various simulation methods and hardware: MPM MC running on GPU (continuous line), non-parallelised MPM MC run on CPU (dashed line) and 1PM MC run on CPU (dotted line).

MSD for non-parallelised MPM MC is about 11.8 times lower than that for the standard 1PM MC because the pairwise additivity gives priority to 1PM MC steps. The situation is, however, completely different if the MPM MC is parallelised and executed on the GPU. One can see that, even with our non-optimised code, the GPU is able to accelerate the MPM MC computation by a factor of 52. Consequently, the MPM MC simulation is about 4.4 times faster than the 1PM MC on a single CPU. The convergence of the configurational energy to its equilibrium value further supports this statement. It is worth mentioning here that, for 4096 particles, we have not used the fast shared memory which has significantly slowed down the computations.

For a complete comparison of 1PM and MPM methods, one should also consider the former method run on the GPU. However, GPU is very unsuitable for 1PM MC, in principle. As it is well known, the full advantage of the GPU architecture can be made use of only if the program is run fully in parallel and as much processor fibres as possible are engaged which, however, cannot be the case of 1PM. Even for a system made up of thousands of particles and the 1PM MC being somehow parallelised, only a very small fraction of available fibres of the processor will be engaged, with the rest being idle. There is therefore no reason to run 1PM on the GPU, and this option has not therefore been considered at all.

We have carried out similar simulations, i.e. the conventional 1PM MC and MPM MC executed on the GPU, for the TIP4P model of water, and the results are shown in Figure 2. As one can see, also in this case, the parallelised MPM MC outperforms the 1PM MC method.

4.2 Structure of the water–methanol mixture

To further demonstrate usability of the MPM MC scheme, we have applied it to two water–methanol mixtures differing in the use of different models: (1) the pairwise-additive TIP4P and KBFF models and (2) the polarisable BSV model and the pairwise-additive KBFF model, with the total number of particles $N = 500$; the simulations were performed at constant N, P and T, at various concentrations, ambient conditions ($T = 298.15$ K, $P = 101{,}325$ Pa), and with the potential cut-off $R_c = 9$ Å

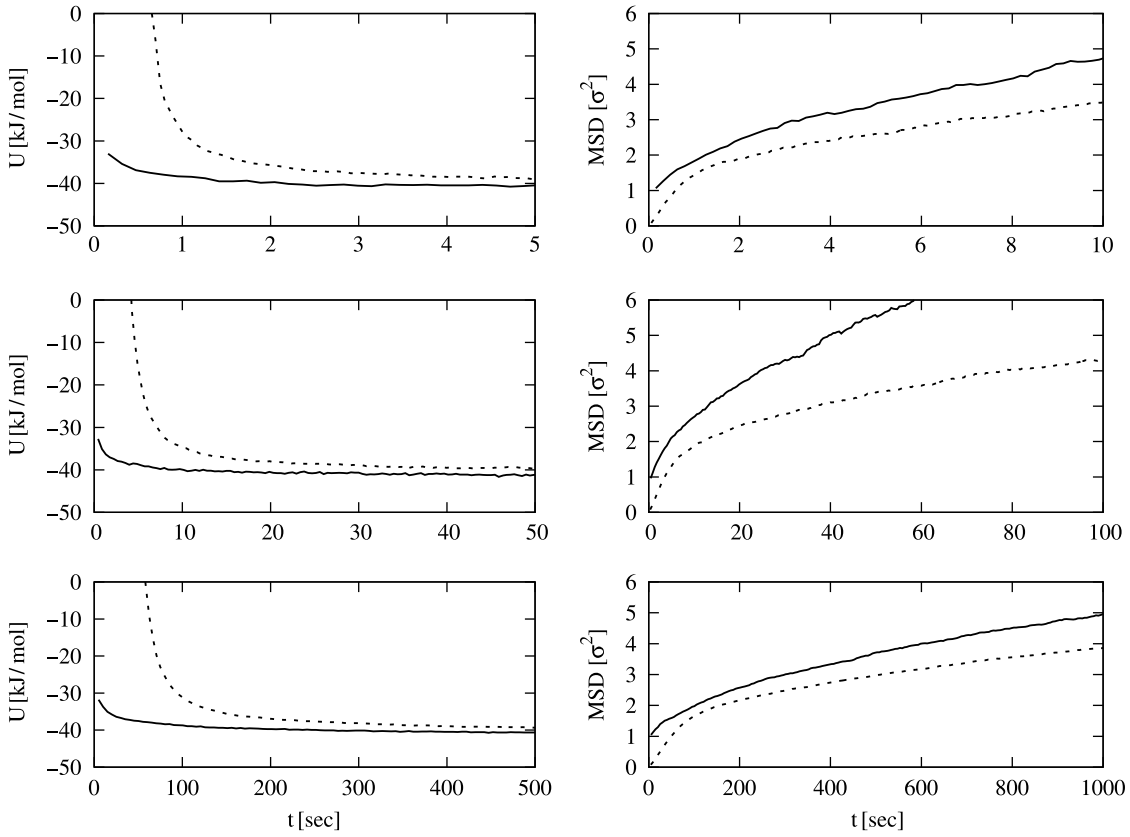

Figure 2. The same properties as in Figure 1 for the TIP4P model of water at ambient conditions.

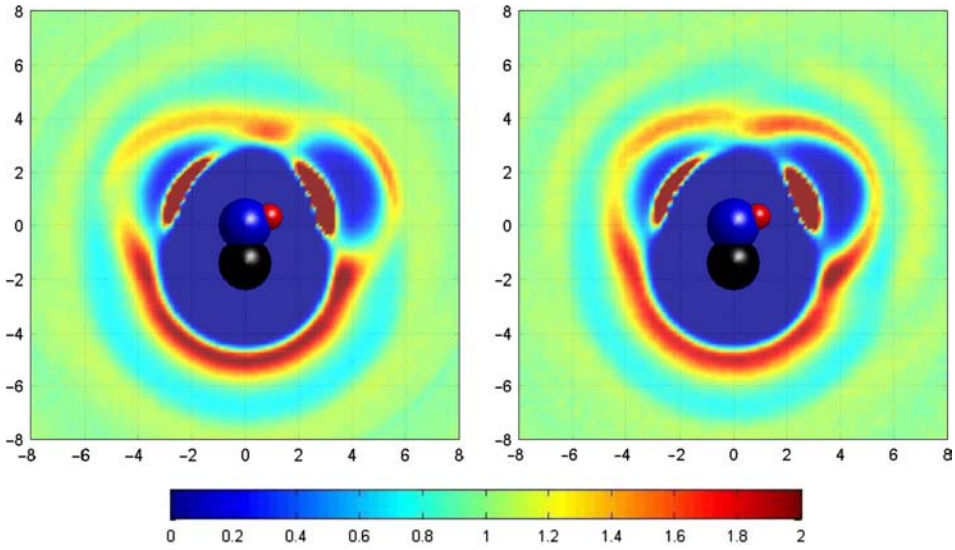

Figure 3. Water–methanol mixture at ambient conditions and $x_{\mathrm{MeOH}} = 0.1$ modelled by the BSV + KBFF potentials (left) and TIP4P + KBFF potentials (right). The spatial distribution of the water oxygen site around the methanol reference molecule, sliced by the plane going through the methanol oxygen site.

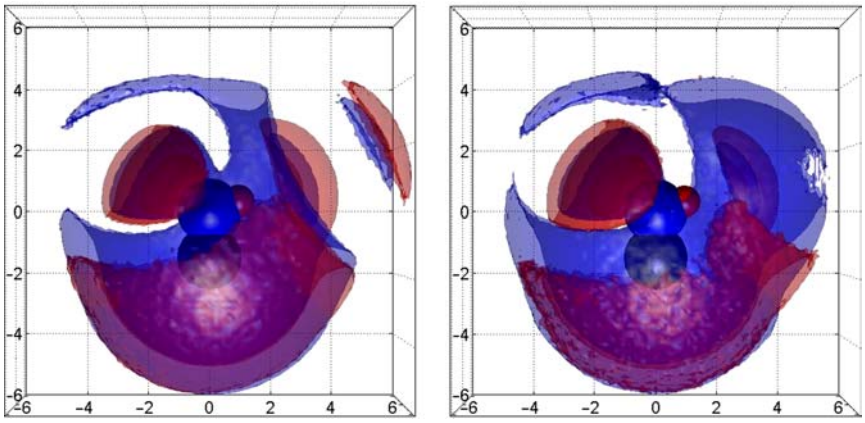

Figure 4. The same as Figure 3 for the SDFs of the water sites around the methanol reference molecule, visualised using isosurfaces formed by all the points where SDF = 1.3: oxygen site (blue), hydrogen site (red) and methyl site (black).

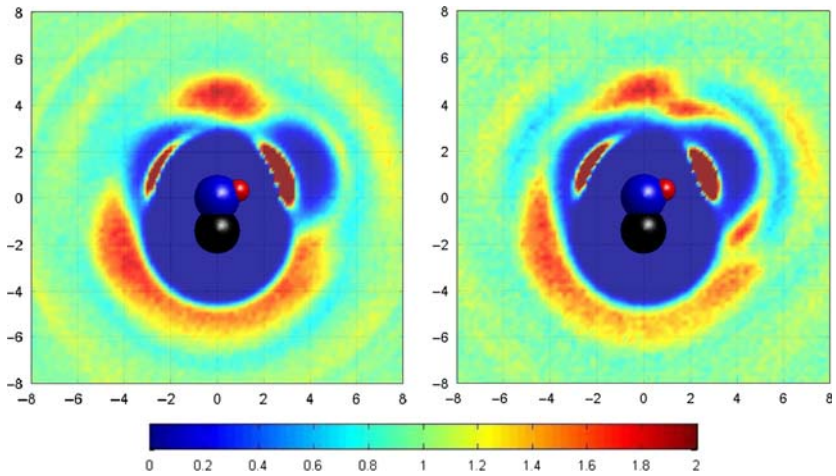

Figure 5. The same as Figure 3 for the methanol oxygen site around the methanol reference molecule, sliced by a plane going through the methanol oxygen site.

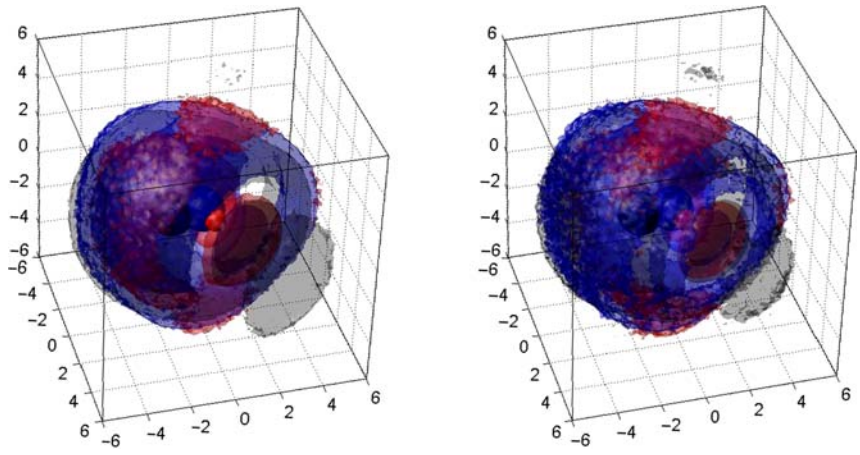

Figure 6. The same as Figure 4 for the methanol sites around the methanol reference molecule and isosurfaces with SDF = 1.4.

[both reaction field potentials and forces smoothed over the interval (8.8 and 9 Å)]. In the induced dipoles iteration step, criterion (14), we always use $m = 5$.

The used SDFs provide a very detailed insight into the local structure around a reference molecule. First, we should mention their ability to detect and illustrate even very weak density deviations throughout the space surrounding the reference molecules. Another interesting fact is that the rate of their decay with increasing intermolecular separation is, in contrast to the common radial distribution functions, much slower.

Since the goal of this paper is not to study in detail the properties of the water–methanol mixture from the viewpoint of their physical behaviour, we present only some selected results showing the main features and differences resulting from the use of the polarisable and non-polarisable models; such a study will be the subject of another report [29].

In Figure 3, we compare the structure of the mixture modelled by the polarisable and non-polarisable models of water. We show the distribution function of the water oxygen sites sliced by the plane containing all the interaction sites of the reference methanol molecule. At first sight, both the structures are very similar. The regions of the oxygen occurrence, governed mainly by the methyl and oxygen sites, are almost identical for both polarisable and non-polarisable models. The same applies to the first shell around the hydrogen site. However, in the second shell around the hydrogen site, a distinct qualitative difference is observed. In the case of the polarisable model, the oxygen sites of the surrounding water molecules mostly rest at a distance about 4.7 Å from the reference hydrogen site, in a cap-shaped region with its axis going through the oxygen and hydrogen sites of the reference methanol molecule. In the case of the pairwise-additive model, the oxygen sites occur in the same distance from the hydrogen site but mostly in positions that are distant from the oxygen–hydrogen axis.

The situation is better seen in Figure 4, where we show the distribution of all sites of the water molecules using the isosurfaces. It turns out that the mentioned oxygen cap-shaped region observed in the case of the polarisable model is accompanied by a greater hydrogen occurrence region of a similar shape and which is about 0.5 Å farther from the reference methanol molecule.

In Figure 5, we further show another example of a qualitative difference in the structure of the studied mixtures. In this case, it is the distribution of the water molecule oxygen sites around the methanol reference molecule. Also, in this case, the structures are very similar and a difference is found again only in the second shell around the hydrogen site. Two high-density regions appear in the slice of the distribution function obtained using the pairwise-additive model but these are absent in the case of the polarisable one. This difference is located in the same position as the one shown in Figures 3 and 4. The spatial visualisation using isosurfaces in Figure 6 discloses the existence of an increased oxygen density ring-shaped feature, although the methanol–methanol SDF suffers from statistical errors because the number of the methanol–methanol molecular pairs, and thus also of the contributions to the SDF calculations, is not very high for low methanol concentrations.

5. Conclusions

In this paper, we have tried to demonstrate advantages of the MPM MC method when compared to the conventional 1PM MC, and a feasibility to write a code for the graphics cards even for complex intermolecular potential models. As for the former, the efficiency is evident for systems with non-additive interactions, but it may also be efficient for simple models if available modern hardware and the parallelisable character of MPM MC are made use of. Since this is our first application using the GPU, we have focused rather on feasibility than on efficiency. The performance of the MPM MC scheme can be further enhanced if the multiprocessor's shared memory and coalesced memory access are utilised (NVIDIA CUDA Programming Guide, http://www.nvidia.com/object/cuda_develop.html). For a fair and more complete assessment of the MPM MC, a comparison with the other available MC method, which also employs MPM, hMC, should be made. In general, advantages of the present MPM MC are that (1) it is applicable, unlike hMC, to any potential model (e.g. to potentials with discontinuity) and (2) it seems technically less demanding than hMC. On the other hand, an advantage of hMC is that codes for molecular dynamics are readily available, both as commercial of freeware products.

As a consequence of the fast performance of the MPM code, we have managed to obtain, within a reasonably short time, information on the structure in the system with the polarisable model and did detect differences when compared to the non-polarisable model. These differences may be responsible for the different thermodynamic behaviour of both models, and they will be the subject of further detailed study. A similarly complex, albeit pairwise additive, system is the one made up of large flexible molecules, e.g. polymers. Preliminary considerations and test runs indicate that, also in this case, the MPM MC scheme may turn out to be a very efficient tool without any need to resort to specially devised complex moves and tricks. Further application of the MPM MC method will proceed along this line and the results will be published in due course.

Acknowledgement

This work was supported by the Grand Agency of the Academy of Sciences of the Czech Republic (Grant No. IAA400720802).

References

[1] N. Metropolis, A.W. Rosenbluth, M.N. Rosenbluth, A.H. Teller, and E. Teller, *Equation of state calculation by fast computing machines*, J. Chem. Phys. 21 (1953), pp. 1087–1092.

[2] D. Frenkel and B. Smit, *Understanding Molecular Simulation*, Academic Press, San Diego, CA, 2002.

[3] M.P. Allen and D.J. Tildesley, *The Computer Simulation of Liquids*, Clarendon Press, Oxford, 1987.

[4] W.W. Wood, *Monte Carlo method*, in *Physics of Simple Liquids*, H.N.V. Temperley, J.S. Rowlinson, and G.S. Rushbrook, eds., North Holland, Amsterdam, 1968, Chap. 5, pp. 115–230.

[5] P.J. Rossky, J.D. Doll, and H.L. Friedman, *Brownian dynamics as smart Monte Carlo simulation*, J. Chem. Phys. 69 (1978), pp. 4628–4633.

[6] W. Chapman and N. Quirke, *Metropolis Monte Carlo simulation of fluids with multiparticle moves*, Physica B 131 (1985), pp. 34–40.

[7] R. Vogelsang and C. Hoheisel, *A Monte Carlo FORTRAN 200 programme for the determination of static properties of liquids vectorized to run on the Cyber 205 vector processing computer*, Comput. Phys. Commun. 46 (1987), pp. 209–216.

[8] S. Gupta, *Comments regarding Monte Carlo simulation of classical fluids on general purpose supercomputers*, Comput. Phys. Commun. 50 (1988), pp. 293–295.

[9] S.J. Singer, *Multiple Monte Carlo moves: Algorithm for solid with free-energy determination*, Comput. Phys. Commun. 59 (1990), pp. 463–470.

[10] S. Duane, A.D. Kennedy, B.J. Pendleton, and D. Roweth, *Hybrid Monte Carlo*, Phys. Lett. B 195 (1987), pp. 216–222.

[11] B. Mehling, D.W. Heermann, and B.M. Forrest, *Hybrid Monte Carlo method for condensed-matter systems*, Phys. Rev. B 45 (1992), pp. 679–685.

[12] C. Desgranges and J. Delhommelle, *Phase equilibria of molecular fluids via hybrid Monte-Carlo Wang–Landau simulation: Applications to benzene and n-alkanes*, J. Chem. Phys. 130 (2009), pp. 244109–244109-7.

[13] T. Aleksandrov, C. Desgranges, and J. Delhommelle, *Vapor–liquid equilibria of copper using hybrid Monte Carlo Wang–Landau simulations*, Fluid Phase Equilibr. 287 (2010), pp. 79–83.

[14] B. Chen and J.I. Siepmann, *Monte Carlo algorithms for simulating systems with adiabatic separation of electronic and nuclear degrees of freedom*, Theor. Chem. Acc. 103 (1999), pp. 87–104.

[15] M. Předota, P.T. Cummings, and A.A. Chialvo, *Pair approximation for polarization interaction: Efficient method for Monte Carlo simulations of polarizable fluids*, Mol. Phys. 99 (2001), pp. 349–354.

[16] M. Předota, P.T. Cummings, and A.A. Chialvo, *Pair approximation for polarization interaction and adiabatic nuclear and electronic sampling method for fluids with dipole polarizability*, Mol. Phys. 100 (2002), pp. 2703–2717.

[17] P. Jedlovszky and J. Richardi, *Comparison of different water models from ambient to supercritical conditions: A Monte Carlo simulation and molecular Ornstein–Zernike study*, J. Chem. Phys. 110 (1999), pp. 8019–8031.

[18] F. Moučka, M. Rouha, and I. Nezbeda, *Efficient multiparticle sampling in Monte Carlo simulations on fluids: Application to polarizable models*, J. Chem. Phys. 126 (2007), pp. 224106–224108.

[19] C. Pangali, M. Rao, and B.J. Berne, *On a novel Monte Carlo scheme for simulating water and aqueous solutions*, Chem. Phys. Lett. 55 (1978), pp. 413–417.

[20] F. Moučka and I. Nezbeda, *Multiple-particle sampling in Monte Carlo simulations on fluids: Efficiency and extended implementations*, Mol. Simul. 35 (2009), pp. 660–672.

[21] F. Moučka and I. Nezbeda, *Partial molar volume of methanol in water: Effect of polarizability*, Coll. Czech. Chem. Commun. 74 (2009), pp. 559–563.

[22] D. Gonzales-Salgado and I. Nezbeda, *Excess properties of aqueous mixtures of methanol: Simulation versus experiment*, Fluid Phase Equilibr. 240 (2006), pp. 161–166.

[23] W.L. Jorgensen, J. Chandrasekhar, J.D. Madura, R.W. Impey, and M.L. Klein, *Comparison of simple potential functions for simulating liquid water*, J. Chem. Phys. 79 (1983), pp. 926–935.

[24] J. Brodholt, M. Sampoli, and R. Vallauri, *Parametrizing a polarizable intermolecular potentials for water*, Mol. Phys. 86 (1995), pp. 149–158.

[25] S. Weerasinghe and P.E. Smith, *A Kirkwood–Buff derived force field for methanol and aqueous methanol solutions*, J. Phys. Chem. B 109 (2005), pp. 15080–15086.

[26] F.J. Vesely, *N-particle dynamics of polarizable Stockmayer-type molecules*, J. Comput. Phys. 24 (1977), pp. 361–371.

[27] M. Neumann and O. Steinhauser, *The influence of boundary conditions used in machine simulations on the structure of polar systems*, Mol. Phys. 39 (1980), pp. 437–454.

[28] I.M. Svishchev, A.Yu. Zassetsky, and P.G. Kusalik, *Solvation structures in 3D*, Chem. Phys. 258 (2000), pp. 181–189.

[29] F. Moučka and I. Nezbeda, *Water–methanol mixtures: Non-polarisable versus polarisable models*, J. Chem. Phys., submitted for publication.